

A Streptavidin–Protein Cage Janus Particle for Polarized Targeting and Modular Functionalization

Peter A. Suci,^{†,§} Sebyung Kang,^{†,‡} Mark Young,^{*,†,§} and Trevor Douglas^{*,†,‡}

Center for BioInspired Nanomaterials, Department of Chemistry & Biochemistry, and Department of Plant Sciences and Plant Pathology, Montana State University, Bozeman, Montana 59717

Received April 30, 2009; E-mail: tdouglas@chemistry.montana.edu

The incorporation of Janus particles into the repertoire of nanoscale building blocks adds a new level of control to supramolecular assembly.^{1–3} Asymmetric motifs are employed by natural systems to orchestrate targeted pathogenesis.⁴ With respect to biomedical applications of engineered systems, toposelective modification of multifunctional nanoplatfoms promises the realization of sophisticated designs for targeting cells with drugs and imaging agents.^{5–7} Here we demonstrate the potential for using toposelective modification to assemble new types of targeting nanoplatfoms by docking the universal coupling protein, streptavidin (StAv), onto a restricted region of the surface of a small (9 nm diameter) protein cage. This is accomplished without inducing extensive cross-linking and aggregate formation. The resulting StAv-functionalized Janus particles have the potential to be used to control the orientation of the nanoplatfoms targeted to a cell surface.⁶ In addition, the StAv–biotin couple provides an ideal molecular adaptor for extending asymmetric (polarized) supramolecular assembly. An obvious application in this respect is modular asymmetric functionalization with an antibody, providing a method for easily adapting a multifunctional nanoplatfom to target a diverse set of cell epitopes. To demonstrate this “plug and play” application, StAv-functionalized nanoplatfoms were coupled to a biotinylated monoclonal antibody (mAb) and used to target a microbial pathogen, *Staphylococcus aureus*.

Protein cages are nanoplatfoms composed of monomeric protein subunits^{8,9} that have been engineered to transport both diagnostic^{10,11} and therapeutic¹² agents. We used a protein cage, LiDps (the DNA-binding protein from *Listeria innocua*), as a template for fabrication of the StAv-functionalized nanoplatfom.^{13,14} LiDps was genetically modified to add a tetrapeptide (KLFC) to each of the 12 protein subunit C-termini, which are presented on the exterior surface of the assembled protein-cage shell. A surface-masking approach was used to toposelectively biotinylate the KLFC LiDps construct (Scheme 1).^{15,16} Biotin was tethered to the sulfhydryl of the C-terminal Cys residue on each of the KLFC peptides via a PEO₂ spacer. Mass spectrometry data indicated that three of the 12 protein subunits were biotinylated (Figure 1S in the Supporting Information).¹⁶ The StAv-functionalized nanoplatfoms were assembled by exposing the toposelectively biotinylated KLFC LiDps immobilized on the thiol-reactive beads used for the surface masking to an aqueous solution of StAv and were then released from the beads by reduction of the disulfide linkages with 25 mM DTT and purified by size-exclusion chromatography (Scheme 1 and Figure 2S). The resulting StAv–KLFC LiDps preparation incorporates StAv as a coupling moiety, and the nine Cys residues asymmetrically positioned on the nonbiotinylated protein subunits are available for further functionalization.

Scheme 1. Surface-Masking Approach Used to Toposelectively Biotinylate the KLFC LiDps Construct and Couple StAv to the Janus Particle (Purple Subunits, Free Sulfhydryl; Sky-Blue Subunits, Biotinylated; Green Subunits, Fluorescently Tagged)



The StAv/KLFC LiDps preparation consisted of a well-dispersed nanoparticulate suspension containing a substantial portion of StAv–nanoplatfom heterodimers. Heterodimer structures consisting of one StAv per protein cage were observed by transmission electron microscopy (TEM) (Figure 1 and Figure 3S). The mean hydrodynamic radius of the StAv-functionalized nanoplatfom preparation, as determined by dynamic light scattering, was 6.8 nm (diameter 13.6 nm) (Figure 4S). In view of their highly anisotropic shape, this relatively large hydrodynamic radius relative to that of the unmodified LiDps protein cage (9 nm diameter) is consistent with a population composed primarily of heterodimers.¹⁷ The incorporation of StAv into the StAv-functionalized nanoplatfom was confirmed by following StAv–biotin-directed dual-layer assembly of multilayer films using a quartz crystal microbalance (Figure 5S).

The StAv-functionalized nanoplatfoms can be used for modular functionalization with a biotinylated mAb. We demonstrated this capability by targeting the microbial pathogen *S. aureus* with this adaptor complex coupled to a biotinylated mAb that binds to protein A expressed on the cell surface (Figure 2).

Figure 2b shows *S. aureus* cells targeted with the mAb–StAv–KLFC LiDps complex, which was labeled with fluorescein maleimide

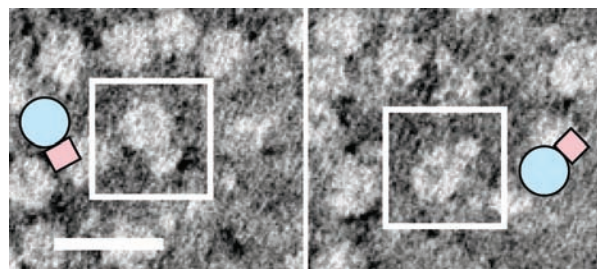


Figure 1. Structure of StAv-functionalized nanoplatfoms observed by TEM. Shapes that would be expected for two orthogonal projections of a heterodimer cross section are indicated. Cartoons are drawn to scale. Scale bar is 20 nm.

[†] Center for BioInspired Nanomaterials.

[§] Department of Plant Sciences and Plant Pathology.

[‡] Department of Chemistry & Biochemistry.

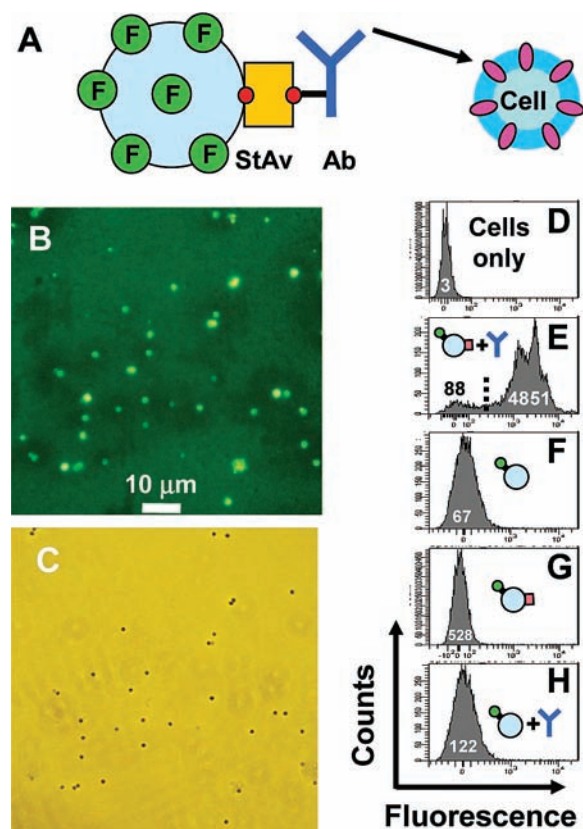


Figure 2. Cells targeted with the fluorescently tagged mAb–StAv–cage preparation. (A) Schematic illustration of the targeting strategy: the biotinylated mAb was targeted against protein A, a surface protein expressed by *S. aureus*. (B) Epifluorescence image of targeted cells. (C) Transmitted image of the same field as in B, showing all the cells in the field of view. (D–H) Distribution of fluorescence among cell populations for targeted cells and negative controls (flow cytometry data): (D) nontargeted cells; (E) cells targeted with the fluorescently tagged mAb–StAv–cage preparation; (F) cells exposed to fluorescently tagged KLFC LiDps; (G) cells exposed to fluorescently tagged StAv-functionalized KLFC LiDps; (H) cells exposed to fluorescently tagged KLFC LiDps and mAb. Histograms are the results of 10^3 counts, and numbers indicate mean fluorescence intensities.

(Scheme 1). Flow cytometry histograms of populations consisting of 10^3 cells corroborated the microscopic data and indicated that targeting was dependent on the presence of all the components required to assemble into a StAv–KLFC LiDps heterodimer, with a low level of nonspecific labeling when either the StAv or mAb was omitted (Figure 2d–h and Figure 6S).

In summary, we have synthesized a StAv-functionalized protein cage that can serve as a “plug and play” nanoplatform for coupling to a biotinylated functional group. We envision an immediately useful application of this construct will be as a modular unit to which a targeting Ab can be easily attached via the StAv–biotin couple. Antibodies offer an almost unlimited range of specific targeting moieties, and affinities can be enhanced significantly by biomolecular engineering.¹⁸ The construct may also be useful in two-step sequential pretargeting applications where it is desirable to transport the cargo subsequent to the Ab-binding step.¹⁹ Our strategy requires that the nanoplatform be toposelectively biotinylated

before coupling to StAv. Attempts to use a symmetrically biotinylated protein-cage nanoplatform for StAv coupling resulted in extensive cross-linking and aggregate formation, as expected. Although StAv can be covalently linked to biomolecules,²⁰ the substantial effort directed at creating StAv chimeric fusion proteins suggests that this route is labor-intensive for many protein–StAv pairs.^{21,22} Furthermore, our strategy of using toposelectively biotinylated nanoplatforms as the starting material not only facilitates coupling of StAv to the nanoplatform but also enables a measure of control over the stoichiometry of the coupling. Thus, the final nanoplatform is sufficiently functionalized for targeting while leaving many addressable sites available for designing functional activity or cargo transport into the system. Finally, the asymmetrical positioning of the StAv coupling protein provides an opportunity for realizing imaging or drug delivery strategies that rely on a polarized orientation of targeted functional groups with respect to the cell surface.

Acknowledgment. This research was supported in part by grants from the National Science Foundation (CBET-0709358), the Office of Naval Research (N00014-03-1-0692), the DOE-Basic Energy Sciences (DE-FG02-07ER46477), and the Human Frontier Science Program (RGP61/2007).

Supporting Information Available: Experimental details and Figures 1S–6S. This material is available free of charge via the Internet at <http://pubs.acs.org>.

References

- Edwards, E. W.; Wang, D. Y.; Mohwald, H. *Macromol. Chem. Phys.* **2007**, *208*, 439–445.
- Perro, A.; Reculosa, S.; Ravaine, S.; Bourgeat-Lami, E. B.; Duguet, E. J. *Mater. Chem.* **2005**, *15*, 3745–3760.
- Walther, A.; Muller, A. H. E. *Soft Matter* **2008**, *4*, 663–668.
- Wosten, H. A. B. *Annu. Rev. Microbiol.* **2001**, *55*, 625–646.
- Roh, K. H.; Martin, D. C.; Lahann, J. *Nat. Mater.* **2005**, *4*, 759–763.
- Roh, K. H.; Yoshida, M.; Lahann, J. *Langmuir* **2007**, *23*, 5683–5688.
- Roh, K. H.; Yoshida, M.; Lahann, J. *Materialwiss. Werkstofftech.* **2007**, *38*, 1008–1011.
- Douglas, T.; Young, M. *Science* **2006**, *312*, 873–875.
- Uchida, M.; Klem, M. T.; Allen, M.; Suci, P.; Flenniken, M.; Gillitzer, E.; Varnness, Z.; Liepold, L. O.; Young, M.; Douglas, T. *Adv. Mater.* **2007**, *19*, 1025–1042.
- Uchida, M.; Flenniken, M. L.; Allen, M.; Willits, D. A.; Crowley, B. E.; Brumfield, S.; Willis, A. F.; Jackiw, L.; Jutila, M.; Young, M. J.; Douglas, T. *J. Am. Chem. Soc.* **2006**, *128*, 16626–16633.
- Suci, P. A.; Berglund, D. L.; Liepold, L.; Brumfield, S.; Pitts, B.; Davison, W.; Oltrogge, L.; Hoyt, K. O.; Codd, S.; Stewart, P. S.; Young, M.; Douglas, T. *Chem. Biol.* **2007**, *14*, 387–398.
- Flenniken, M. L.; Liepold, L. O.; Crowley, B. E.; Willits, D. A.; Young, M. J.; Douglas, T. *Chem. Commun.* **2005**, 447–449.
- Ilari, A.; Stefanini, S.; Chiancone, E.; Tsernoglou, D. *Nat. Struct. Biol.* **2000**, *7*, 38–43.
- Kang, S.; Oltrogge, L. M.; Broomell, C. C.; Liepold, L. O.; Prevelige, P. E.; Young, M.; Douglas, T. *J. Am. Chem. Soc.* **2008**, *130*, 16527–16529.
- Klem, M. T.; Willits, D.; Young, M.; Douglas, T. *J. Am. Chem. Soc.* **2003**, *125*, 10806–10807.
- Kang, S.; Suci, P. A.; Broomell, C. C.; Iwahori, K.; Kobayashi, M.; Yamashita, I.; Young, M.; Douglas, T. *Nano Lett.* **2009**, *9*, 2360–2366.
- Wilkins, D. K.; Grimshaw, S. B.; Receveur, V.; Dobson, C. M.; Jones, J. A.; Smith, L. J. *Biochemistry* **1999**, *38*, 16424–16431.
- Barderas, R.; Desmet, J.; Timmerman, P.; Meloan, R.; Casal, J. I. *Proc. Natl. Acad. Sci. U.S.A.* **2008**, *105*, 9029–9034.
- Goldenberg, D. M.; Sharkey, R. M.; Paganelli, G.; Barbet, J.; Chatal, J. F. *J. Clin. Oncol.* **2006**, *24*, 823–834.
- Feng, K.; Kang, Y.; Zhao, J. J.; Liu, Y. L.; Jiang, J. H.; Shen, G. L.; Yu, R. Q. *Anal. Biochem.* **2008**, *378*, 38–42.
- Laitinen, O. H.; Airenne, K. J.; Raty, J. K.; Wirth, T.; Yla-Herttuala, S. Y. *Lett. Drug Des. Discovery* **2005**, *2*, 124–132.
- Sano, T.; Vajda, S.; Cantor, C. R. *J. Chromatogr., B* **1998**, *715*, 85–91.

JA9035187